https://doi.org/10.5194/egusphere-2025-695
Preprint. Discussion started: 20 March 2025

Is the summer aerosol over the Arctic controlled by regional atmospheric circulation or ice conditions? Trends and Future Implications

Caroline Leck[1], Jost Heintzenberg[2], Tiina Nygård[3], Tuomas Naakka[3]

[1]Department of Meteorology and Bert Bolin Centre for Climate Research, Stockholm University, Stockholm, 106 91, Sweden
[2]Leibniz Institute for Tropospheric Research, Leipzig, 04318, Germany
[3]Finnish Meteorological Institute, PB 503, Helsinki, 00101, Finland

Correspondence to: Caroline Leck (lina@misu.su.se)

Abstract. The study is based on aerosol particle size distributions measured during five Swedish icebreaker research expeditions to the central Arctic Ocean at latitudes of 85ºN and above in 1991, 1996, 2001, 2008, and 2018. These aerosol data were complemented with hourly back trajectories, daily maps of sea ice, and ER5-data on atmospheric and oceanic variables. Regional atmospheric circulation regimes (nodes) based on the method of Self Organizing Maps (SOMs) were investigated as potential controllers of inner Arctic aerosol sources. Despite substantial climate change, the most prominent nodes were not connected to regional aerosol-source-related differences and did not vary systematically over the study period. Instead, the seasonal course of sea ice melt and freeze-up strongly affected the shape of the aerosol size distributions in the atmosphere closest to the surface. In particular, high sub-Aitken concentrations occurred during the freeze-up of new ice. These high concentrations of newly formed particles were interpreted as deriving from frost flower formation during late summer/autumn. With ERA5 and ice data until 2023, the study period was extended to a total of 33 years, during which the significant increases in sea and air temperatures nearly doubled the favorable ice conditions for new particle formation ≥85ºN, lengthening both melt and freeze-up parts of the illuminated Arctic approximate by 10 days. Whereas the sum effect of counteracting processes during the ice melt on the airborne biogenic Arctic aerosol in a warming climate is unclear, the net impact of the changing freeze-up of sea ice is expected to enhance the airborne biogenic Arctic aerosol in late summer/autumn.

1 Introduction

Over the past three decades, earlier ideas about a pristine summer Arctic (≥80ºN), practically devoid of aerosol sources, had to be revised. In the marginal ice zone, sea spray concentrations in terms of the number and mass of organic and inorganic components are the highest and decrease by nearly an order of magnitude due to frequent and efficient wet scavenging processes during the first 1-2 days of advection from the open sea into the pack ice (Bigg and Leck, 2001;Heintzenberg et al., 2006;Leck and Persson, 1996;Leck et al., 2013;Nilsson and Leck, 2002).

If the air is advected over the pack ice for extended periods (typically more than four days) since its last contact with the open ocean, the concentrations of sea spray number and mass increase again, but at a significantly lower level compared to that observed along the ice edge zone of the Greenland Sea-Fram Strait area (Nilsson et al., 2001). Nevertheless, it has been proposed that local sources during the melt period in the pack ice contribute to sea spray residuals from the surface microlayer (SML) of open leads[1], produced by bubble bursting, generating film and jet drops, respectively (Heintzenberg et al., 2015;Held et al., 2011;Leck et al., 2002;Leck and Bigg, 2005;Salter et al., 2016).

[1] Open leads are openings of sea water in pack ice and characteristically form long, narrow channels, 1-100m wide and up to kilometers long.

https://doi.org/10.5194/egusphere-2025-695
Preprint. Discussion started: 20 March 2025

Moreover, Leck et al. (2002) found that smaller film drop particles mainly consist of organics whereas larger jet drop particles are primarily sea salt. The latter become more numerous relative to the film drops only in winds exceeding 12 ms^{-1}. This is a rare condition in the inner Arctic as generally low wind speeds prevail (70% of the time less than 6 m/s, Tjernström et al., 2012). The open lead source of sea spray organic material has subsequently been demonstrated to be biogenic and to consist of marine polymer gels[2] (Orellana et al., 2011). High Arctic data also showed ample organic material in surface waters for polymer gel assembly, mainly at the surface microlayer (SML) interfaces, interacting with the atmosphere (Matrai et al., 2008). Bigg and Leck (2008) noted that bubbles in the water column effectively transfer surface ocean gel matter to the air. Their walls may be composed mostly of surface-active material, draining seawater before bursting at the sea-air interface. Film drops may not contain water; they hold only the gel network's liquid.

The transition from the melting period into late summer/autumn commences with the initiation of ice formation, which restricts the exchange of nascent sea spray with the atmosphere when the open lead is freshly frozen. Nonetheless, the formation of frost flowers and bubbles at the water-ice boundary may allow the transfer of matter from the SML rich in polymer gels. The initial layer of ice is referred to as greased ice, which resembles an oily film. This layer rapidly solidifies into thin sheets in calm waters and accumulates through processes of rafting and ridging (Comiso, 2010). Saline brine becomes trapped within the ice crystals, resulting in a brine-wetted surface on the newly formed ice. Due to its high salt concentration, brine remains in a liquid state and does not freeze. Recently formed thin surface ice dissipates heat, leading to convective mixing and localized gas saturation variations, resulting in bubble formation beneath. The duration since its last exposure to open air can influence bubble generation. Ongoing freezing at the water-ice interface might promote the release of gas from the frozen water, helping maintain saturation in the cooled liquid.

Typically, during high-pressure atmospheric systems with calm winds and cold temperatures (< -8° C), brine can migrate upward or be expelled from the sea surface under the new ice, forming highly saline centimeter-scale frost flowers (Galley et al., 2015;Perovich and Richter-Menge, 1994). Young sea ice contains organic material from microorganisms, exudates, and detrital particles (Andrea et al., 2007). Formation-stress concentrates exudates in the ice, forming polymer gels by diatoms and bacteria (Andrea et al., 2007;Krembs et al., 2002). Bowman and Deming (2010) found that frost flowers have higher levels of bacteria and extracellular polymer gels than brines, young ice, or water. Their findings suggest that frost flowers allow SML and young sea ice to interact chemically with the atmosphere, potentially serving as a source of polymer gels. Yet, the process by which frost flowers generate airborne aerosol particles is not fully understood. One significant proposed method involves mechanical fracture. Additionally, two other possible mechanisms include brine being directly expelled from the frost flower structure and particles formed by pressurizing the brine channel during the freezing phase of the frost flowers (Alvarez-Aviles et al., 2008).

Our previous studies also demonstrated the occurrence of small, recently formed particles in the inner summer Arctic (Covert et al., 1996;Heintzenberg et al., 2006;Heintzenberg and Leck, 2012;Heintzenberg et al., 2015;Leck and Bigg, 1999). One explanation for their occurrence was based on condensible vapors that may be emitted or formed over the sunlit Arctic, allowing the nucleation of new particles from the gas phase if, one, gas phase concentrations are high enough and are sustained for sufficiently long times, and, two, existing particulate surfaces are sufficiently low to prevent vapor condensation on existing particles. It has been shown in recent findings in the inner Arctic that reactions between iodic acid and sulfuric acid often result in the formation of new particles, which is particularly notable during the freeze-up period (Baccarini et al., 2020).

Finally, small particles may also be generated in the atmosphere by fragmentation of primary particles. There are suggestions that airborne polymer gels might break down, resulting in smaller particles (e.g., Karl et al., 2012;Lawler et al., 2021;Leck and

[2] Marine polymer gels are exudates from phytoplankton, ice algae, and bacteria consisting of Ca^{2+}/Mg^{2+} cross-linked polysaccharides that bind together small particulates and organic molecules such as amino acids, peptides, proteins, and lipids. (Orellana et al., 2021).

https://doi.org/10.5194/egusphere-2025-695
Preprint. Discussion started: 20 March 2025

Bigg, 2010). The fragmentation of marine gels likely occurs due to the repeated condensation and dissipation of fogs or clouds, as evidenced by the strong indication of a condensed phase-related aerosol source (Heintzenberg et al., 2006). This process could account for the previously noted simultaneous production of multi-sized aerosol particles smaller than approximately 50 nm in diameter, which contrasts with the traditionally observed chemical and/or condensational growth of atmospheric particles. However, it remains unclear whether the marine gel shrank due to UV radiation cleavage, reversible volume phase transitions caused by changes in temperature and pH, or a combination of these factors (Orellana et al., 2021). Thus, the breakup of gel aggregates in the atmosphere remains an unresolved research question (Lawler et al., 2021).

Over the past few decades, climate change has affected the Arctic more than any other region on Earth. The temperature north of 66.5° N has risen almost four times faster than the global average in recent decades (Rantanen et al., 2022), calculated for the years 1979-2012. This effect is referred to as "Arctic amplification." One of the most noticeable consequences is the alarming reduction in the extent and mass of sea ice, which occurs in all seasons but most dramatically in late summer when the sea ice extent has its annual minimum (Meier et al., 2014). The regional aerosol potentially plays a significant role in regulating the surface energy budget through aerosol-to-cloud interactions. It may help counteract some of the warming effects over the Arctic pack ice area (Mauritsen et al., 2011).

The air mass analyses of Heintzenberg et al. (2015) showed that the summer aerosol over the pack ice has different potential source regions along its periphery. Consequently, in the present study, the question of whether regional-scale atmospheric circulation patterns are controlled by regional aerosol sources over the inner Arctic is pursued. Thus, in a first step, a synopsis of all aerosol number size distributions accumulated during the past five ice breaker (I/B) *Oden* expeditions, 1991-2018, was compared to the inner Arctic 85-90° N (Leck et al., 1996;Leck et al., 2001;Leck et al., 2019;Tjernström et al., 2004;Tjernström et al., 2014) using synoptic pressure charts and the SOMs (Self Organizing Maps) method. The most significant number of observations occurred while the I/B *Oden* was moored to an ice floe in the inner pack ice area between 85-90° and drifted passively during the ice melt into autumn freeze-up conditions, roughly beginning with August through late September. The SOM method uses unsupervised learning to determine generalized patterns in data and, as such, clusters a large volume of synoptic pressure fields according to similar large-scale circulation distributions. Each timestep of the input data will belong to one of the resulting circulation regimes called nodes. The SOM method will also provide circulation distributions or regimes (nodes), of e.g., horizontal moisture transport, total cloud water, radiation, evaporation, and temperature at the surface. The nodes were subsequently linked to the number size distributions of all aerosol number size distributions accumulated during the past five I/B *Oden* expeditions.

The minimal ice cover by late summer follows the gradual creation of melt ponds and reduction of dry ice caused by solar energy input and rising air temperatures, which commence as the sun rises above the horizon in March. This period is referred to as "melt." During the start of new ice formation, called "freeze-up," the first ice layer forms when the sea temperature is close to its freezing point, dropping below ≈ -1.8° C. As mentioned above, this first layer of greased ice rapidly solidifies into thin sheets, thickening through rafting and ridging processes until it is fully frozen (Comiso, 2010). Connecting air mass analyses with sea ice cover indicated that broken ice conditions strongly affected the formation of new particles (Heintzenberg et al., 2015). The second focus of the present study was stimulated by these findings, in which the detailed seasonal evolution of the sea ice is employed to understand its impact on aerosol sources and the shape of their size distributions over the summertime Arctic pack ice area. The daily ice maps were used to analyze sea ice conditions during “melt” and “freeze-up”. This analysis was conducted for each year from 1991 to 2018. The information from the ice maps was then linked to the number size distributions of all aerosol number size distributions accumulated during the past five I/B *Oden* expeditions.

In the last part of the study, the SOMs that were available for all summers 1991-2018, ice maps, and sea surface and atmospheric temperature data from ERA5 (the fifth generation (European Centre for Medium-Range Weather Forecasts, ECMWF) until 2023 were combined in two geographic regions. The inner Arctic region ≥85ºN was compared with the marine region between 78º and 82ºN. With marginal ice and advanced summer melt, the latter region can reference today's conditions

https://doi.org/10.5194/egusphere-2025-695
Preprint. Discussion started: 20 March 2025

that may govern the inner Arctic within a few decades, as indicated in Fig. 1 of Wassman and Reigstad (2011). This extensive data set explored potential long-term trends and implications of atmospheric and ice conditions for the future of Arctic aerosol sources in summer.

2 Methods

2.1 Self-Organizing Maps and Surface Air and Ocean Temperatures

The European Centre for Medium-Range Weather Forecasts (ECMWF) Reanalysis v5 (ERA5) mean sea level pressure (MSLP) fields were clustered using the Self-Organizing Maps (SOM) method to identify the Arctic's main large-scale atmospheric circulation regimes. The SOM method, developed by Kohonen (2001), is an unsupervised learning method, i.e., a machine-learning approach, to identify generalized patterns in data. The method has previously proven valuable in atmospheric applications (Nygård et al., 2019;Thomas et al., 2021), providing physically meaningful composites of field patterns.

The MSLP data was used at 12-hour intervals and covered days from August to September 1991–2018 as input data for the SOM analyses. As a first step, the MSLP data were re-gridded to an equal-area grid. Then, the SOM algorithm created an initial SOM array containing six nodes with random reference vectors of an equal dimension as the input MSLP data. After that, each input data vector was compared with the reference vectors, and the reference vectors most similar to the input data vector were adjusted towards the input data vector. This was repeated until the reference vectors converged. Finally, the SOM algorithm provided an organized SOM array of MSLP patterns, having the most similar nodes (i.e., circulation regimes) next to each other. However, in this paper, composites of the MSLP fields associated with each node were presented, not the output reference vectors of the SOM analysis. For a more detailed description of the SOM method, please see Kohonen (2001) and Hewitson and Crane (2002).

The choice of the SOM output array size is always, to some extent, subjective (Alexander et al., 2010). The results for a 2 x 3 array and a 3 x 4 array were compared, and it was concluded that the 2 x 3 array should be proceeded with. These six nodes in the 2 x 3 array sufficiently represent the range of large-scale circulation patterns in the Arctic. It is also beneficial for only a few nodes to be present when our aerosol observational data was later associated with the circulation regimes; this will ensure that sufficient observational data is available to be associated with each node to provide statistically representative results.

Several variables of ERA5 (Hersbach et al., 2020;Hersbach, 2023, (last accessed 2024-10-31)) reanalysis were investigated for an overview of the meteorological conditions linked to the circulation regimes. ERA5 is a state-of-the-art global atmospheric reanalysis that applies a four-dimensional variational data assimilation method to assimilate various observations. Uncertainties in the representation of MSLP fields by ERA5 are assumed to be minor, as in global reanalyses in general (Nygård et al., 2021). However, uncertainties in ERA5 radiation, especially cloud variables, may be considerably more significant (Nygård et al., 2021).

In this study, the mean 10-m wind vectors, temperatures (2 meters and 850hPa), vertically integrated moisture vectors, total cloud water, net LW radiation, and temperature at the surface in ° C were separately calculated for each of the six MSLP circulation regimes. In addition, an extended period of two meter-air temperatures from the ERA5 analyses for August and September of 1991-2023 was also utilized. Arctic-wide average temperature values north of 85ºN were calculated ±6h about each time step of the SOMs to interpret SOMs, sea ice, and aerosol data.

Half-day mean (06 – 18 and 18 – 06) 2m temperature (T2m) and Sea Surface Temperature (SST) values were calculated from hourly ERA5 data. Areal mean time series were constructed for two areas ≥85° N and in the latitude band 78° N – 82° N from half-day mean values. Only ocean areas where the land fraction is less than 0.1 were included in the calculation. T2m was calculated in the ERA5 assimilation cycle. Still, since the atmospheric model used to produce the ERA5 reanalysis does not include ocean model SSTs, these are provided as input for assimilation. Two datasets have been used to provide SST values

https://doi.org/10.5194/egusphere-2025-695
Preprint. Discussion started: 20 March 2025

for ERA5. Before September 2007, SST for ERA5 was supplied by the HadISST2 dataset (Titchner and Rayner, 2014), and from September 2007 onward, it was provided by the OSTIA dataset (Good, 2022).

2.2 Aerosol measuring systems and platforms

Number-size distributions of aerosol particles have been measured on I/B *Oden* on all five Arctic expeditions. From 1991 through 2008, basically, the same type of differential mobility analyzers were deployed, albeit with varying upper and lower size limits and number of steps in particle diameter. Details of the respective instrument setups and measures to minimize the risk of contamination from the platform are described in Covert et al., (1996), Leck et al., (2001), and Heintzenberg et al., (2012).

In 2018, a new type of aerosol spectrometer was added to a scanning differential mobility analyzer that extended the size range down to one nanometer (Baccarini et al., 2020;Karlsson and Zieger, 2020). For the present study, the hourly average size distributions from the five expeditions were harmonized by interpolating them on a common array of 50 logarithmically equidistant diameters from 3.37 to 900 nm. Previous studies (Covert et al., 1996;Heintzenberg and Leck, 2012) had shown that the surface aerosol in the inner Arctic exhibited number size distributions as a combination of several modes. These included nucleation modes below 10 nanometer, ultrafine particle modes below 25 nm, Aitken modes with a maximum between 25 and 80 nm, and accumulation modes above 80 nm in diameter. Consequently the harmonized size distributions were fitted to an array of two to six log-normal size distributions between one and 1000 nm following a procedure outlined in Whitby and McMurry (1997). Only aerosol data ≥ 85º N were utilized for our focus on the inner Arctic. The exact periods and numbers of used hourly aerosol data are collected in Table 1. Aerosol data coverage in relation to "melt" and "freeze-up" is shown in Fig. A1 in the Supplement.

Table 1: Start and end date and time (UTC) of hourly I/B *Oden* aerosol data utilized in this study in 1991, 1996, 200, 2008, and 2018, and the number of utilized hourly averaged distributions (Scans) ≥85° N after screening for possible ship pollution (total 2476).

Year	Start date	End date	Scans
1991	23 August	20 September	560
1996	1 August	9 September	715
2001	1 August	24 August	503
2008	10 August	3 September	411
2018	15 August	16 September	287

2.3 Air-mass back trajectories

Hourly five-day air-mass back trajectories were calculated arriving at I/B *Oden*. They cover each hour of the utilized size distribution data. The trajectories were based on the meteorological fields kindly made available by the US National Weather Service's National Center for Environmental Prediction (NCEP). Before 2005, the trajectories were based on NCEP/NCAR reanalyzed meteorological fields with 2.5° × 2.5° resolution (https://www.ready.noaa.gov/gbl_reanalysis.php, last accessed 2023-09-08). After 2005, the calculations were based on the Global Data Assimilation System (GDAS1). In horizontal grids of 1° × 1° resolution, meteorological parameters are stored every three hours with a vertical grid spacing of 23 pressure surfaces between 1000 and 20 hPa. Vertical layers one through 25 hPa separates five layers. All higher layers (with the exception of the top layer) are separated by 50 hPa, (Kanamitsu, 1989). The HYSPLIT-model for trajectory calculation, (Stein et al., 2015), analyzes the meteorological inputs to determine the appropriate internal vertical model resolution so that there are sufficient levels to interpolate all the meteorological input without skipping data due to insufficient vertical resolution.

For the present study, the trajectory ensemble option of HYSPLIT was used. It starts multiple trajectories from a given starting location to estimate the uncertainty associated with the center point trajectory. Each member of the trajectory ensemble is calculated by offsetting the meteorological data by a fixed grid factor (one grid meteorological grid point in the horizontal

https://doi.org/10.5194/egusphere-2025-695
Preprint. Discussion started: 20 March 2025

and 0.01 sigma units in the vertical). This results in 27 members for all possible offsets in X, Y, and Z (https://www.ready.noaa.gov/hypub-bin/trajtype.pl, last accessed 2024-02-22). As it is recommended that the starting height exceed 250 m for optimal ensemble configuration, a height of 300 m was chosen as the arrival height over I/B *Oden*.

2.4 Sea ice and open water

Daily Arctic ice maps were downloaded from the U.S. National Snow and Ice Data Center database every day from 1991 through 2023. North of ≈ 87ºN, a circular mask covers the irregularly shaped data gap around the North Pole caused by the ice-sensing satellites' orbit inclination and instrument swath. After 2007, improved satellite technology reduced this pole gap to >89ºN. At each trajectory point, the ice map nearest in time was utilized to identify up to four pixels of this ice map within 50 km of the trajectory point. The average open-water information taken over these nearest pixels was added to the respective trajectory point.

Within the periods of the nodes in the SOMs, probability frequency distributions (pdf) of open water under the back trajectories of the respective particle size distributions were accumulated. These pdfs yield estimates of aerosol-related ice conditions during the different large-scale flow conditions represented by the nodes. The information from the ice maps was also utilized directly in specific statistics of ice conditions ≥85ºN by relating the number of pixels with given ice conditions, e.g., ≥ 20 % open water, to the total number of pixels ≥85ºN. By doing this for August and September of each of the 33 years 1991-2023, long-term statistics and trends of ice conditions relevant to the present study were constructed.

3 Results

Six characteristic summer atmospheric Mean Sea Level Pressure (MSLP) patterns or circulation regimes were identified as results of the SOM analysis, which can be seen in Fig. 1a. The mean 10-m wind vectors associated with the circulation regimes can also be seen in Fig. 1b. The MSLP circulation patterns, corresponding anomalies, and wind vectors were calculated based on the August-September 1991-2018 average. The six circulation regimes represent distinct pressure conditions, particularly over Greenland, Alaska, and northern parts of Russia. The circulation regimes that occurred most commonly during 1991-2018 were nodes 2, 3, and 6 (see Fig. 2a), and those nodes were selected for further investigation.

Circulation regime 2 is characterized by high pressure over Greenland and anomalously low MSLP over northern Eurasia (Fig. 1a and Appendix Fig. A2). In this regime, the central Arctic Ocean experienced a relatively strong airflow primarily from the direction of the Beaufort, Chukchi, and East Siberian Seas towards the Fram Strait and the Greenland Sea. The air mass was anomalously warm, as indicated by the roughly 2° C temperature anomaly at 850 hPa level, over the Beaufort, Chukchi, and East Siberian Seas (Fig. 3b, left side chart). However, this warm air mass did not extend to Greenland and Barents Seas, which have negative temperature anomalies at the 850 hPa level. Circulation regime 2 was also associated with an anomalously large amount of cloud water over the ice-covered Arctic Ocean (Fig 3d, left side chart), which was linked to enhanced net longwave radiation at the surface (Fig 3e, left side chart). The combination of large-scale temperature advection and radiative heating by the clouds was associated with anomalously high temperatures of 2m (T2m) over most of the Arctic Ocean (Fig. 3f, left side chart).

The main feature of circulation regime 3 was the anomalously low pressure over Greenland, which steers the airflow from the northern North Atlantic towards the North Pole and further towards the Canadian Arctic Archipelago (Fig. 1a-b and Appendix Fig. A2). This regime efficiently transported large amounts of heat and moisture from the northern North Atlantic to the Arctic (Fig. 3c, middle chart). The air mass at 850 hPa was anomalously warm over Greenland, Barents, and Kara Seas (Fig. 3b, middle chart). This also led to an anomalously high amount of cloud water and enhanced net longwave radiation over the Greenland and Barents Seas (Fig. 3d-e, middle chart), which, together with the warm air advection, explained the anomalously warm T2m conditions (Fig. 3f, middle chart).

https://doi.org/10.5194/egusphere-2025-695
Preprint. Discussion started: 20 March 2025

Circulation regime 6 (Fig. 3a-e, right side charts) was characterized by weak pressure gradients and, thus, by very weak large-scale winds over the Arctic Ocean. Advection of heat and moisture is weak, meaning that the Arctic conditions were not affected mainly by large-scale horizontal transport, but the conditions were somewhat more locally driven. This regime was associated with an anomalously small amount of cloud water, which enabled enhanced cooling by the longwave radiation. In particular, the T2m was anomalously low (Fig. 3f, right side chart).

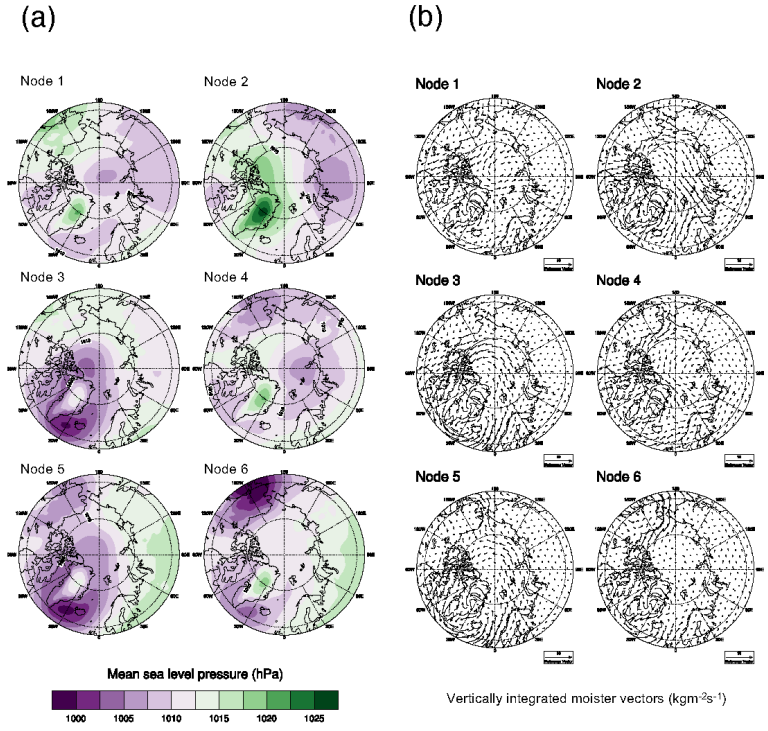

Figure 1: (a) Mean sea-level pressure and **(b)** wind vector at 10m height above ground level circulation regimes (2x3 nodes): calculated for August-September, including all years from 1991 to 2018.

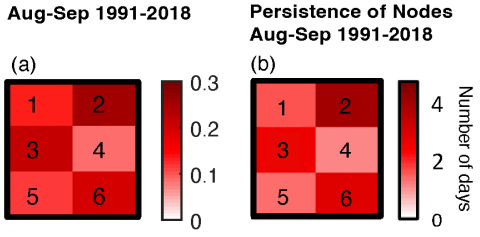

Figure 2: **(a)** August to September circulation regimes of occurrence for the six nodes displayed in Figure 1; calculated for all years from 1991 to 2018, **(b)** the mean persistence of nodes (in days).

https://doi.org/10.5194/egusphere-2025-695
Preprint. Discussion started: 20 March 2025

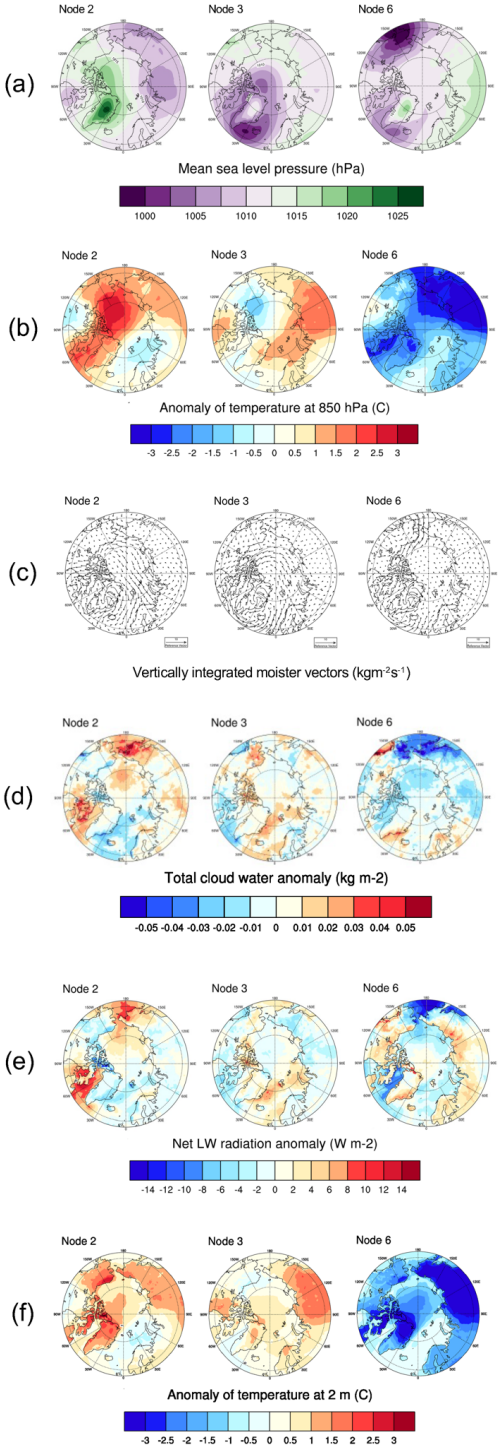

250

Figure 3: (a) Mean sea-level pressure in hPa, **(b)** the anomaly of temperature in ° C for 850 hPa, **(c)** vertically integrated moister vectors in kg m^{-2} s^{-1}, **(d)** total cloud water anomaly in kg m^{-2}, **(e)** net LW radiation anomaly in W m^{-2}, **(f)** and anomaly of temperature at the surface in ° C for circulation regimes (nodes) 2,3 and 6; were calculated for August-September, including all years from 1991 to 2018.

https://doi.org/10.5194/egusphere-2025-695
Preprint. Discussion started: 20 March 2025

4 Linking particle size distributions to SOMs and conditions of "melt" and "freeze-up"

Whenever available, the hourly size distribution data of the five I/B *Oden* cruises were averaged ±6h around the SOM times before being grouped into the six SOM nodes. When the statistics of SOM occurrence were reduced to the five expedition years in Fig. 4, the dominance of nodes 2, 3, and 6 in Fig. 2 was maintained.

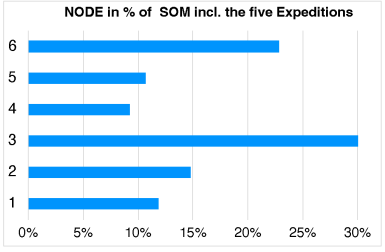

Figure 4: Probabilities of the occurrence of the six nodes in Figure 2 in August and September for the five expedition years: 1991, 1996, 2001, 2008, and 2018.

The I/B *Oden* expeditions all started in the developing "melt" and ended before "freeze-up" was complete (cf Appendix Fig. A1). Near-surface temperatures dropping below zero characterize the transition from "melt" to the start of "freeze-up." Tjernström et al. (2012) suggested using a threshold of - 2° C for this transition. The net surface energy balance could also indicate melting and freezing; as the surface temperature is practically at zero, a negative net surface energy balance indicates freezing, and a positive one provides energy for melting. However, in this study, the -2° C temperature threshold was augmented by adjusting it with onboard observations of ice formation during the individual cruises. With this procedure, hourly timelines were formed with conditions of "melt" and "freeze-up" for each expedition. The aerosol observations were then grouped according to the two ice conditions. The start of "freeze-up" was estimated to be August 18, 19, 19, 21, and 27 for 1991, 1996, 2001,2008, and 2018 data sets, respectively.

Statistics of the occurrence of the nodes in the two ice conditions were collected in Fig. 5. Figure 5a indicates that melt conditions were mainly associated with circulation regime 3. This was a consequence of the strong advection of heat and moisture from the North Atlantic and enhanced longwave radiative heating at the surface due to warm and moist air and excessive cloud water. The freeze-up was most commonly linked to circulation regime 6 as seen in Fig. 5b, where there was very weak horizontal transport of heat and moisture, and the meteorological conditions were more locally driven. Regime 6 enabled enhanced radiative cooling at the surface. The combination of low wind speeds, calm waters that limit the sea ice movement, and efficient radiative cooling created favorable circumstances for the freeze-up.

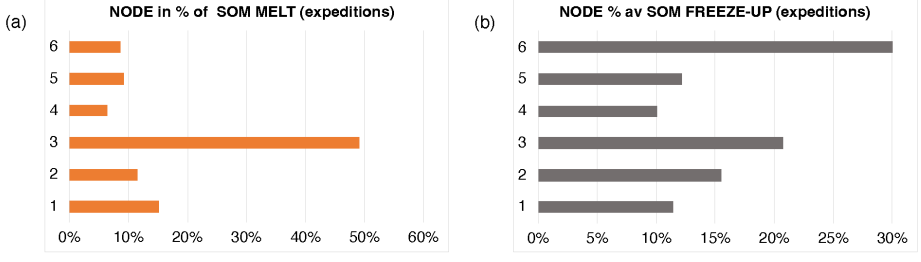

Figure 5: Probabilities of the occurrence of the six nodes in Figure 2 in August and September for the five expedition years: 1991, 1996, 2001, 2008, and 2018. The data is sorted into **(a)** "melt" and **(b) "**freeze-up".

https://doi.org/10.5194/egusphere-2025-695
Preprint. Discussion started: 20 March 2025

In addition to melting and freezing (i.e., thermodynamic) conditions, the circulation regimes have dynamic impacts on sea ice. The pack ice in the central Arctic Ocean moves in response to air stress, water stress, sea surface tilt, and the Coriolis force. The geostrophic wind influences approximately half of the long-term ice motion, while the other half is attributed to mean ocean circulation. Over shorter time scales, more than 70 % of ice velocity variability can be accounted for by the geostrophic wind (Thomdike and Cheung, 1977).

The wind-driven Arctic ice circulation consists of the Beaufort Gyre, a clockwise circulation north of Alaska that spawns low winds, and the Transpolar Drift Stream (Timmermans and Marshall, 2020). The latter moves ice from Siberia across the Arctic basin to the North Atlantic off the east coast of Greenland. Sea ice transport towards the Fram Strait follows. Wind vector circulation regime 2 (Fig. 1b) can thus significantly affect the central Arctic Ocean's Sea ice concentration by inducing sea ice transport via the Fram Strait. On the other hand, the winds associated with regime 3 (Fig. 1b) tend to mechanically push and pack the sea ice towards the central Arctic Ocean and the coast of the Canadian Arctic Archipelago. However, the sea ice field responds relatively slowly to the atmospheric circulation field, and therefore, it was relevant to how persistent the circulation regimes were at the time. Persistent, long-lasting occurrences of circulation regimes have more potential to modify the sea ice field. As shown in Fig. 2b, regime 2 was the most persistent, lasting on average for 4 days, while regimes 3 and 6 typically prevailed for 3 days, calculated for all years from 1991 to 2018.

In Fig. 6, the pressure regimes of nodes 2, 3, and 6 were compared to average particle size distributions during "melt" and "freeze-up" of the respective nodes for data ≥ 85ºN. Despite strongly differing regional meteorological conditions, all size distributions during "freeze-up" exhibited high particle concentrations in the sub-Aitken region below 30 nm and a secondary mode or at least a concentration shoulder above 100 nm diameter. The high sub-Aitken concentrations were missing during the melt in nodes 3 and 6. In contrast, the size distributions in node 2, also in "melt" indicated strong new particle formation with high nucleation mode concentrations below 10 nm diameter, which will be dealt with below.

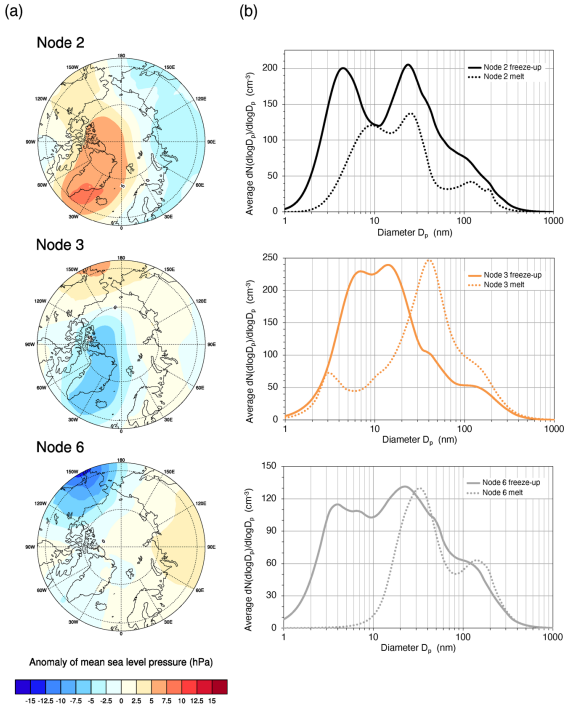

Figure 6: (a) Nodes 2, 3, and 6 surface pressure regimes, **(b)** Average particle size distributions during "melt" and "freeze-up" of the nodes in the left panel. Only aerosol data ≥85ºN are displayed.

https://doi.org/10.5194/egusphere-2025-695
Preprint. Discussion started: 20 March 2025

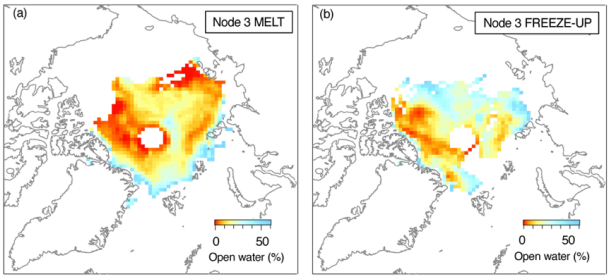

Figure 7: Sea ice coverage under five-day back trajectories in node 3, **(a)** "melt"; **(b)** "freeze-up". Only geocells with ≥30 trajectory points are displayed. No ice data is close to the pole due to the ice-sensing satellites' orbit inclination and instrument swath.

The probability frequency distributions (pdfs) of open water conditions in Fig. 8 show the differences between nodes and ice conditions more clearly than maps. Figure 8a connects to the maps in Fig. 7. It showed very little solid ice in "freeze-up" compared to "melt" and high probabilities for broken-up ice with a distinct peak around 10 % open water. The corresponding pdf maximum lay at 5 % open water in "melt." Both ice conditions exhibit broad shoulders towards 50 % open water, albeit with higher probabilities in freeze-up. Completely open water under the back trajectories occurred in both conditions with about 20 % probability. The pdfs for nodes 2, 3, and 6 in Fig. 8b confirmed and emphasized the widespread occurrence of broken ice during freeze-up for node 3, as shown in Fig. 7b.

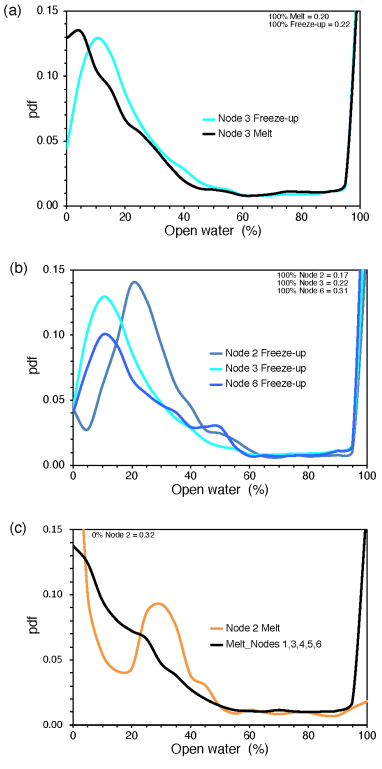

Figure 8: (a) Probability frequency distributions (pdfs) of open water under the back trajectories of node 3 in "melt" and "freeze-up", **(b)** As top panel but for "freeze-up" in nodes 2, 3, and 6, **(c)** As top panel but for node 2 and average conditions during the "melt" of nodes 1, 3, 4, 5, and 6. Probabilities of 0 % and 100 % open water are given as numbers in text boxes.

https://doi.org/10.5194/egusphere-2025-695
Preprint. Discussion started: 20 March 2025

The outlier size distributions of node 2 in Fig. 6b can now be understood by referring to the pdfs for "melt" in Fig. 8c. An estimate of average ice conditions during "melt" was constructed by taking an average of the pdfs of nodes 1, 3, 4, 5, and 6. Figure 8c showed an average decrease from a 14 % probability of solid ice to a low probability of broken ice beyond 50 % open water with a narrow probability extreme of 100 % open water. In node 2, the ice distribution was very different. Solid ice had a 32 % probability, and 100 % open water only 2 %. At the same time, broken ice occurred with frequencies of up to 10 % and a broad peak of around 30 % in open water. Inspecting the expedition years contributing to the aerosol data in the "melt" of node 2 revealed that almost exclusively, the year 1996 controlled the aerosol data in this node during "melt." The persistent, strong, high-pressure system over Greenland and the western Canadian Arctic Archipelago in 1996 led to the early formation of broken ice during "melt." This peculiar situation in 1996 was discussed by Nilsson and Barr (2001).

In conclusion, the shape of particle size distributions, which exhibited high sub-Aitken concentrations, notably below 10 nm in diameter, indicated strong particle formation over the Arctic pack ice area ≥85ºN. These particle sources appeared to be linked to the occurrence of broken ice during "freeze-up" - a condition most commonly associated with Node 6 (cf. Fig. 5b) The combination of low wind speeds, restricted sea ice movement, and effective radiative cooling contributed to favorable freeze-up conditions.

5 Atmospheric and ice conditions in the inner Arctic in summer and early autumn and long-term implications for regional aerosol sources

5.1 Trends of nodes and related ice conditions

SOMs were available for all years 1991-2018. With this more extensive dataset, the potential of the general occurrence of the most significant nodes was explored. Over the years analyzed, there was no systematic variation in the frequency of node occurrences (cf. Table A1 in the Appendix). Therefore, the following discussion disregarded their interannual variation.

Heintzenberg et al. (2015) showed that ice conditions with open water between 10 % and 30 % a few days before air mass arrival at the observation favored aerosol sources, of which the latter will be discussed further within section 5.4. Consequently, a lower limit of 20 % open water was adopted in the general discussion of aerosol sources over the inner Arctic. In the daily ice maps for August and September 1991-2018, the average number of pixels with open water of at least 20 % relative to the total number of pixels north of 85ºN, termed "open water fraction" (OWF), was calculated and plotted as a black line in Fig. 9, which was extended to the end of 2023 for the subsequent discussion of possible trends. The interannual variability of OWF is substantial and appears to be stronger after the shift in 2006. Despite this high variability, open water increases, at least when the time series is divided into two segments: before and after 2006 (cf. Table A1 in the Appendix). This division into two segments is also discussed in detail in Polyakov et al. (2023) describes an Arctic "switchgear mechanism" involving oceanic circulation. The five expeditions' average open water fractions during August and September, marked as filled yellow circles in Fig. 9, show that neither trend nor variability of the black curve could have been assessed with the expedition data only. The interannual variations of OWF are similar in all nodes (2, 3, and 6). Therefore, only the respective curve for the most prominent node, 3, is shown in Fig. 9 (orange line). Beyond that, segment averages of OWF of all three prominent nodes are marked as dotted and dashed lines, shown in Fig. 9. The segment ratios (before and after 2006) for nodes 2, 3, and 6 are 1.6, 2.1, and 1.6, respectively. The most significant ratio was observed for the wind-driven ice circulation associated with node 3 (cf. Fig. 1b), mechanically pushing and packing the sea ice towards the central Arctic Ocean and the coast of the Canadian Arctic Archipelago. As discussed in Chapter 3, this regime would, in addition, have effectively transported significant amounts of heat and moisture from the northern North Atlantic to the inner Arctic with potential impacts on sea ice melt and increased OWF (Mortin et al., 2016).

https://doi.org/10.5194/egusphere-2025-695
Preprint. Discussion started: 20 March 2025

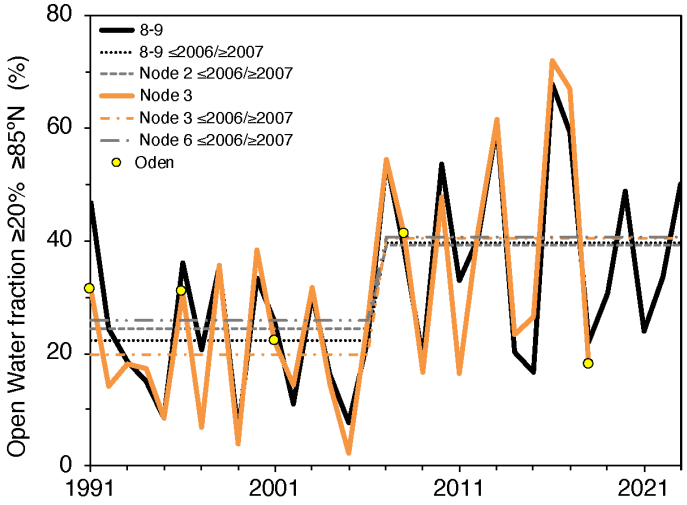

365 **Figure 9:** Average open water fractions ≥ 20 % Open Water (OWF in %) ≥ 85º N during August and September of the years 1991-2023 (full black line) and during regional Arctic circulation according to node 3 (full orange line). Average OWF values during August - September (8-9) and for nodes 2, 3, and 6 before and after 2006 are shown as dotted and dashed lines. Open-water conditions during the five I/B *Oden* cruises are indicated in full yellow circles.

370 Thus, the features of circulation regime 3 were suggested to explain not only the unusually warm (T2m) conditions shown in Fig. 3f (middle chart) but also the most significant change in the average open water fractions (≥ 20 %) ≥85º N during August and September before and after 2006. However, the average value of 1.7 for all three node segment ratios was close to the segment ratio of 1.8 for all August and September days. This similarity leads us to conclude that the different atmospheric circulation patterns of the most prominent nodes (2, 3, and 6) did not significantly lead to differing ice conditions in the inner
375 Arctic, including all years from 1991 to 2018, which deviates from the findings of Thomdike and Cheung (1977) concerning the importance of the geostrophic wind for the movement of the sea ice. Therefore, the atmospheric circulation regimes cannot explain the substantial temporal changes and high interannual variability of ice conditions seen in Fig. 9. In Chapter 4, the locally determined freeze-up was decisive in initiating the conclusion of summer through early autumn, with strong new particle formation subsequently observed on I/B *Oden*. Thus, this study's available atmospheric and oceanic parameters are
380 involved in an aerosol-related trend analysis of the warming-illuminated.

https://doi.org/10.5194/egusphere-2025-695
Preprint. Discussion started: 20 March 2025

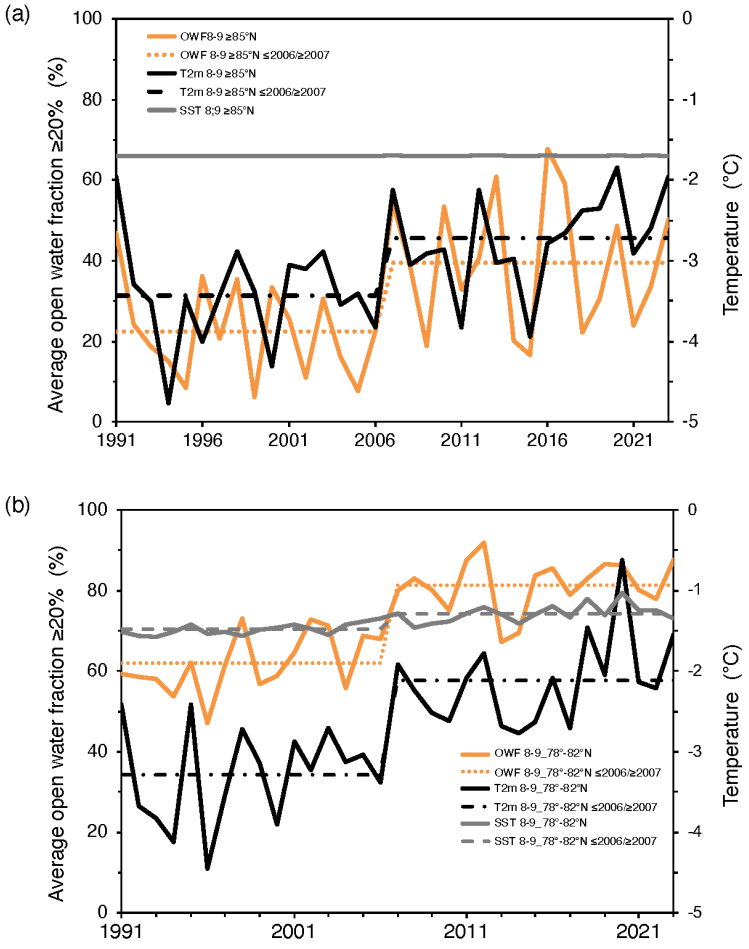

Figure 10: Average values of open water fractions ≥ 20 % (OWT, full orange line), surface air temperatures (T2m, full black line), and sea surface temperatures (SST, full gray line), **(a)** ≥85ºN and in marine regions **(b)** 78º N-82º N for all August/September months from 1991 to 2023. Averages ≤ 2006 and ≥ 2007 are drawn as dotted and dashed lines in the respective colors.

385

5.2 Trends in critical atmospheric and oceanic parameters

The analysis was extended over the whole inner Arctic (≥85° N) using the ice maps and average ERA5 temperatures, and it was extrapolated over all the years, from 1991 to 2023. In Fig. 10, average summer, including September T2m, SST, and OWF values, are collected in the two analyzed Arctic regions during 1991-2023. With substantial interannual variations, nearly all parameters increased with time in both geographic regions (cf. Table A1 in the Appendix). SST ≥85ºN is the exception, for which ERA5 gives fixed values of -1.69° C, which is close to the freezing point of seawater of ca 35 ‰. Average levels in the two segments ≤2006, and ≥2007 are shown as dotted and dashed lines. In these segments, T2m increased on average by 0.7° C and 1.2° C in sectors ≥85º N and 78º N-82º N, respectively, whereas SST in the latter region increased by 0.2° C. The corresponding increases are 1.8 and 1.3, expressed as ratios in OWF, i.e., the open water fraction increased by 80 % and 30 %, respectively. Some correlations of the parameters in Fig. 10 are apparent. The highest values are reached in the region 78º N-82 º N with T2m and OWF showing an r^2=0.7. The following highest correlation concerns T2m and SST in the same region with an r^2=0.6.

https://doi.org/10.5194/egusphere-2025-695
Preprint. Discussion started: 20 March 2025

5.3 Seasonal Changes in Ice Conditions

Employing the ERA5 T2m-data, "melt" and "freeze-up" were delineated according to the following schemes in the two studied geographic regions:

- Start of melt: Day of year (DOY) when regional average T2m rises over -1° C,
- End of melt (start of freeze-up): DOY when regional average T2m sinks below -2° C,
- End of freeze-up: DOY when regional average T2m sinks below -10° C.

The threshold of -1° C for the start of "melt" follows the approach presented in Rigor (2000). As mentioned previously, the value of -2° C for the onset of "freeze-up" was suggested by Tjernström et al. and (2012). When the regional average surface air temperature is considered to be below the somewhat arbitrarily chosen -10° C, the completion of the freeze-up of leads is noted. The variation of the resulting DOY-values over the study period 1991-2023 allows the formulation of trends in the seasonality of the ice cover that may be relevant for regional aerosol sources.

For the region ≥85°N, the temporal development of the three critical DOY-values is depicted in Fig. 11. Over the studied period of 33 years, climate warming yielded systematic trends with an earlier start of melting and later start and end of "freeze-up," albeit with substantial variabilities, being highest at the end of "freeze-up." As a result, the length of both "melt" and "freeze-up" increased with time. For the reference region 78° N-82° N, the directions of the trends are the same, albeit with different slopes.

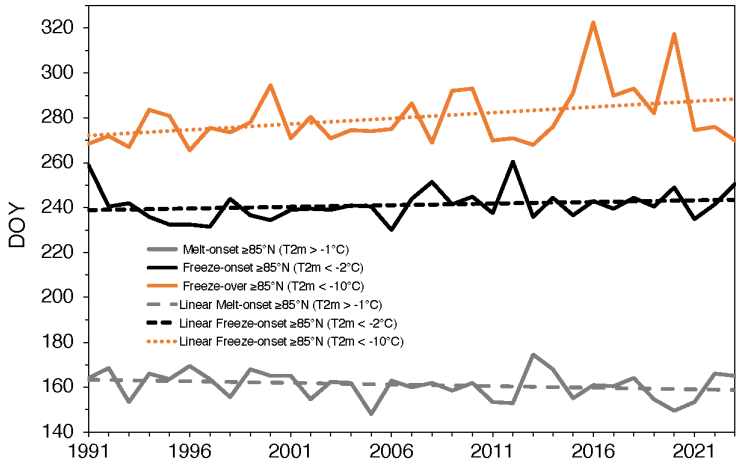

Figure 11: Annual day-of-year-values (DOY) with onset of "melt" (average T2m >-1° C, full gray line), onset of "freeze-up" (average T2m < -2° C, full black line), and end of "freeze-up" (average T2m < -10° C, full orange line) for the region ≥85°N. Respective linear trends are shown as dotted and dashed lines.

Table 2 collects the changes in critical DOY values and length of "melt" and "freeze-up" from 1991 to 2023 for assumed linear developments in the two studied Arctic regions. In 2023, "melt" started ≈5 days earlier than 1991 ≥85°N; "freeze-up" ≈5 days later, ending 16 days later, yielding an increase of ≈9 days for melt and ≈12 days for "freeze-up". Further south, the shifts in critical DOY-vales are more substantial in the reference region. Consequently, the length of "melt" nearly doubled, whereas the length of "freeze-up" is somewhat shorter than further north.

https://doi.org/10.5194/egusphere-2025-695
Preprint. Discussion started: 20 March 2025

Table 2: Changes in critical DOY-values and lengths of "melt" and "freeze-up" from 1991-2023 assuming linear developments in the two regions ≥85ºN, and 78º-82ºN.

Region	Shift of "melt" onset (days)	Shift of onset of "freeze-up" (days)	Shift of end of "freeze-up" (days)	Extension of "melt" (days)	Extension of "freeze-up" (days)
≥85ºN	-4.6	4.7	16.3	9.3	11.6
78-82ºN	-5.3	12.1	22.4	17.4	10.2

5.4 Long-term implications for central Arctic aerosol sources

Before discussing future implications of the observed trends for the central Arctic aerosol, the seasonal variation of particle size distributions is summarized, including all available data (beyond the SOMS discussion). Averages and medians of all data ≥85ºN during "melt" and "freeze-up" are collected in Fig. 12, which emphasizes the substantial differences connected with the two states of ice conditions that showed up in Fig. 6. Under 30 nm, particle diameter average number concentrations during "freeze-up" were up to more than two orders of magnitude higher than during "melt," in particular under 10 nm in diameter, indicative of strong new particle formation. The rather similar median distributions during "melt" and "freeze-up" were interpreted as inner Arctic background, whereas the averages were strongly affected by individual particle formation events.

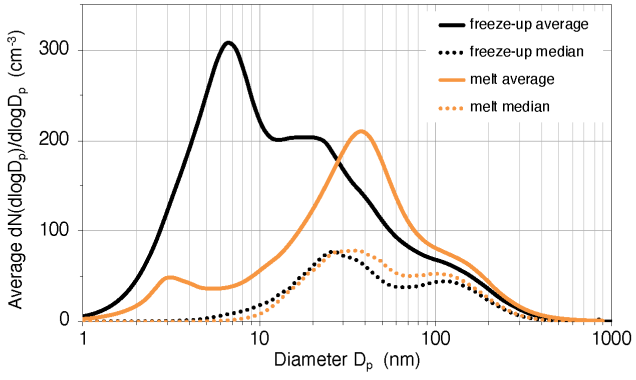

Figure 12: Average and median particle size distributions at ≥85ºN collected over the years 1991, 1996, 2001, 2008, and 2018 during the "melt" and "freeze-up" phases.

Over the study period of 33 years, several atmospheric and oceanic parameters relevant to regional aerosol sources showed significant changes consistent with the known Arctic warming. Assuming an overall linear change (instead of the segment changes ≤ 2006/ ≥ 2007), T2m increased by 1.1° C ≥ 85º N and 2º C in the marginal ice region 78º N-82º N. According to Aslam et al. (2016), these changes must affect the ongoing changes in sea ice distribution, including open water and newly frozen leads, which will significantly impact the ecology of the central Arctic Ocean. Abundant autotrophic and heterotrophic microbiological communities, associated with high concentrations of dissolved and particulate organic matter, grow in sea ice, especially near the ice-water interface of first-year ice (Ewert and Deming, 2013;Thomas, 2010;Vancoppenolle et al., 2013). As such, first-year ice supports more abundant ice-algae communities than multiyear ice, particularly younger ice formed in

https://doi.org/10.5194/egusphere-2025-695
Preprint. Discussion started: 20 March 2025

refrozen leads (Lange et al., 2015). Subsequent enhanced production of dissolved and particulate carbohydrates, including secreted free biopolymers and polymer gels, preconditions the bottom ice layer for optimal habitability and microbial survival: smaller pores (cryoprotectant) of more concentrated brine (osmolyte) and following ice melt (Krembs et al., 2002;Orellana et al., 2011). In areas of first-year ice, both existing and newly formed, the growth of ice algae will be further enhanced by the simultaneous decrease in snow cover, which will allow for increased light exposure (Hezel et al., 2012). Melted sea ice algal biomass, along with dissolved and particulate polymer gels, further aids in aggregate formation into larger sizes, allowing sea-ice organic carbon to reach deeper ocean layers (Riedel et al., 2007). Due to aggregate-inducing gels, increased carbon flux from sea ice may occur with earlier ice melt at the MIZ if grazers feeding on aggregates are absent, leaving less polymer gels accumulating in the upper water column (Carmack and Wassmann, 2006).

In the central Arctic Ocean, marine phytoplankton also produces polymer gels through biological secretions (reviewed by Deming and Young, 2017, and references therein). The stable stratification, usually found in the upper 20 meters of the water column, exhibits a uniform density. Coupled with the significant effects of freshwater (Olli et al., 2007) and water-column seeding of ice algae and nutrients due to melting ice, this environment could also serve as a starting community for phytoplankton growth. This is aided by accumulating dissolved and particulate organic matter in the uppermost water layer during ice melt (Matrai et al., 2008). The dynamics of this accumulation will be influenced by the timing and intensity of both zooplankton and bacterioplankton growth and the resulting interactions within the food web. Whether the particulate and dissolved organic matter is generated *in situ* or advected from outside the open leads, its concentration in the surface microlayer is amplified by physical processes like diffusion and vertical advection caused by buoyant particles and bubbles (Matrai et al., 2008, and references therein).

During the 33 years, this study's results show that OWF nearly doubled ≥85ºN while it increased by ≈50 % in the region 78º N-82º N. In the latter region, SST increased by 0.4ºC, assuming a linear trend; "melt" increased in length by more than a week ≥ 85º N increasing open water areas in sea ice (leads), and by more than two weeks in the region 78º N-82º N. Previous findings on the central Arctic Ocean pack ice and MIZ during "melt", as detailed in the introduction, showed that favorable open water conditions and local emissions of biogenic aerosols derived from the composition of the upper ocean microbial community can change the concentrations (new biogenic particles: Karl et al., 2013;Lawler et al., 2021;Leck and Bigg, 1999;Leck and Bigg, 2010;Orellana et al., 2011) or composition (e.g., organic fragments or coatings on salt particles: Leck et al., 2002;Leck and Bigg, 2005;Leck and Svensson, 2015) of nascent sea spray organic aerosols. Orellana et al. (2011) confirmed that the organic material found in near-surface aerosols behaves similarly to marine polymer gels and that the airborne polymer gels originate from the thin surface microlayer film on open water leads. The extension of "freeze-up" by about ten days with freshly frozen leads restricts the exchange of nascent sea spray with the atmosphere. However, Bowman and Deming (2010) discovered that frost flowers contain significantly more bacteria and extracellular polymer gels than brines, young ice, or water. Their research indicates that a rise in frost flower occurrence could facilitate chemical interactions between sea ice and the atmosphere, acting as an enriched atmospheric source of polymer gels. Iodic acid supports the link between marine biota and aerosols, particularly in new particle formation over central Arctic pack ice during freeze-up (Baccarini et al., 2020). This component derives from the atmospheric photooxidation of iodine, produced by microalgae under sea ice, released by bubbles and frost flowers, from diffusing through sea-ice brine channels (Saiz-Lopez et al., 2015).

Associated with an overall thinning of the sea ice, with earlier and longer "melt", the above discussion makes clear that the resulting formation of more open water leads would increase the illumination of the ocean surface and promote phytoplankton growth, taking advantage of the nutrients already present and seeding by ice-bottom algae due to melting (Arrigo et al., 2012). Ice-algal dissolved organic matter was previously also confirmed to be a significant source of airborne polymer gels (Orellana et al., 2011). However, diminished ice thickness or increased openness of the seas would facilitate more efficient wind mixing of the surface ocean, thereby augmenting the depth of the mixed layer and potentially mitigating algal growth. As detailed above, the extension of "freeze-up" by about ten days in larger areas of open water may increase the occurrence of frost flowers

https://doi.org/10.5194/egusphere-2025-695
Preprint. Discussion started: 20 March 2025

and related gel aerosol sources. Whereas the sum effect of counteracting processes during "melt" on the biogenic Arctic aerosol in a warming climate is unclear, the net effect of the changing "freeze-up" is expected to enhance the biogenic Arctic aerosol in late summer/autumn. In terms of particle size distribution, this may lead to even more prominent sub-Aitken modes than shown in Fig. 12 and discussed in the Introduction. There, the production of small particles was suggested to result from atmospheric fragmentation of micrometer-sized gels by photolysis by UV radiation cleavage or reversible volume phase transitions from temperature and pH changes into short-chain polymers that fail to assemble or form only unstable nanometer-sized gels promoted by long travel times in the air over pack ice or from repeated condensation and dissipation of fog or clouds.

6 Conclusions

The starting point of the present study was aerosol particle number size distributions measured ≥85ºN on five cruises of I/B *Oden* covering the summers of 1991, 1996, 2001, 2008, and 2018, and previous analyses indicating different potential source regions and ice-related factors affecting Arctic aerosol sources. Regional atmospheric circulation regimes (nodes) based on the method of self-organizing maps (SOMs) were investigated as potential controllers of Arctic aerosol sources. Circulation regime 2 featured high pressure over Greenland and low MSLP in northern Eurasia. The central Arctic Ocean experienced strong airflow from the Beaufort, Chukchi, and East Siberian Seas towards the Fram Strait and Greenland Sea. Circulation regime 3 displayed low pressure over Greenland, directing the airflow from the northern North Atlantic to the North Pole and Canadian Arctic. Circulation regime 6 showed weak pressure gradients, causing extremely light large-scale winds across the Arctic Ocean. Despite substantial climate change, the three most prominent nodes were not connected to regional source-related differences and did not vary systematically throughout the study period. Instead, the seasonal course of sea ice melt and freeze-up appeared to affect the shape of the aerosol size distributions significantly. In particular, high sub-Aitken concentrations occurred during the "freeze-up", most commonly associated with the low wind, restricted sea ice movement, and effective radiative cooling conditions of node 6. The high concentrations of newly formed particles measured during "freeze-up" were interpreted as deriving from frost flower formation during this time of the year.

Based on the understanding that ice conditions and their seasonal course are considered major controllers of Arctic aerosol sources, the study was extended to cover all years from 1991 to 2023 to enable speculations about changing aerosol source conditions in the warming Arctic climate. With daily ice maps and sea surface and atmospheric temperatures from the ERA5 database, long-term changes in ice conditions were explored. Over the 33 years of the study, the significant increases in sea and air temperatures nearly doubled the favorable ice conditions for new particle formation ≥85ºN, lengthening both "melt" and "freeze-up" parts of the illuminated Arctic by more than a week. Whereas the sum effect of counteracting processes during the ice melt season on the airborne biogenic Arctic aerosol in a warming climate is unclear, the net effect of the changing the freeze-up of sea ice is expected to enhance the airborne biogenic Arctic aerosol in late summer/autumn. The consequences of the foreseen seasonal changes in biogenic aerosol sources in the inner Arctic remain to be investigated. The strong aerosol-cloud-climate connection would require regional model simulations that take up a possible doubling of airborne biogenic particle numbers during the freeze-up and an unknown net source change during the melt season.

https://doi.org/10.5194/egusphere-2025-695
Preprint. Discussion started: 20 March 2025

Appendix A

Table A1: Statistics and two-tailed statistical tests of significant changes ≤2006 versus ≥2007 of node occurrence (node 1-6), average August/September temperature (T2m) ≥85ºN, and 78ºN-82ºN, sea surface temperature (SST) 78N-82ºN, open water fraction (OWF) ≥ 20 % ≥ 85º N, and 78º N-82º N, median value of first day-of-year (DOY) with average T2m ≥ 85º N >-1 ºC, median value of first day-of-year (DOY) with average T2m 78º N-82º N > -1º C, median value of latest day-of-year (DOY) with average T2m ≥ 85º N sinking < -2º C, median value of latest day-of-year (DOY) with average T2m 78 ºN-82º N sinking < -10º C, median value of latest day-of-year (DOY) with average T2m 78º N-82º N sinking < -10º C, length of melt period ≥ 85º N, length of melt period 78º N-82º N, length of freeze-up period ≥ 85º N, length of freeze-up period 78º N-82º N. The changes are considered significant if P(≤t) two tail is less than 5 %.

Parameter	Unit	Mean ≤2006	Variance ≤2006	Mean ≥2007	Variance ≥2007	P(T≤t) two tail	Change significant?
Node 1	n.a.	0.127	0.008	0.150	0.007	0.560	no
Node 2	n.a.	0.251	0.013	0.253	0.015	0.970	no
Node 3	n.a.	0.228	0.005	0.194	0.015	0.400	no
Node 4	n.a.	0.099	0.002	0.067	0.003	0.096	no
Node 5	n.a.	0.100	0.003	0.068	0.003	0.110	no
Node 6	n.a.	0.193	0.011	0.199	0.010	0.870	no
T2m_8-9, ≥ 85° N	n.a.	-4.5	16.7	-3.6	12.5	3.32E-13	yes
T2m_8-9, 78° N-82° N	n.a.	-3.3	9.0	-2.1	4.6	3.03E-44	yes
SST, 78° N-82° N	n.a.	-1.5	0.005	-1.3	0.012	9.70E-07	yes
OWF, ≥ 20 % ≥ 85° N	n.a.	22	138	40	267	0.002	yes
OWF, ≥ 20 % 78° N-82° N	n.a.	62	54	81	42	5.50E-9	yes
DOYmin, > -1° C ≥ 85° N	n.a.	162	36	160	41	0.370	no
DOYmin, 78° N-82° N	n.a.	163	16	161	29	0.170	no
DOYmax,< - 2° C ≥ 85° N	n.a.	239	47	243	43	0.038	yes
DOYmax,< -2° C 78° N-82° N	n.a.	241	21	248	47	0.002	yes
DOYmax, < -10° C ≥ 85° N	n.a.	275	51	285	261	0.038	yes
DOYmax < -10° C 78° N-82° N	n.a.	277	22	290	115	1.70E-4	yes
Melt, ≥ 85° N	n.a.	74	78	79	128	0.200	no
Melt, 78° N-82° N	n.a.	78	51	87	117	0.007	yes
Freeze-up, ≥ 85° N	n.a.	37	133	41	309	0.338	no
Freeze-up, 78° N-82° N	n.a.	35	31	41	81	0.030	yes

https://doi.org/10.5194/egusphere-2025-695
Preprint. Discussion started: 20 March 2025

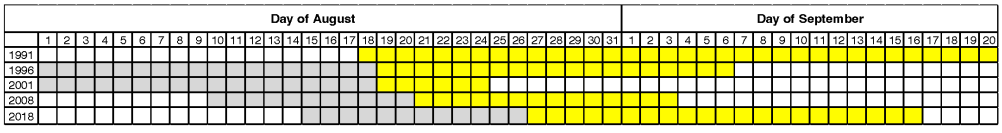

Figure A1: Overview of available number-size distributions of aerosol particles measured on I/B *Oden* during five Arctic expeditions, covering days in August and September in 1991, 1996, 2001, 2008, and 2018. Gray days represent "melt", and yellow days represent "freeze-up". Days without data are indicated by white fields.

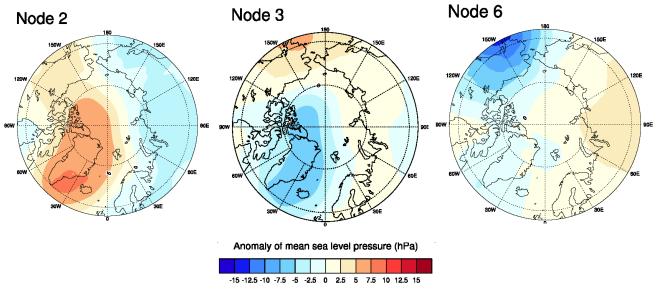

Figure A2: Anomaly of mean sea-level pressure in hPa for circulation regimes (nodes) 2, 3, and 6, calculated for August-September of all years from 1991 to 2018.

https://doi.org/10.5194/egusphere-2025-695
Preprint. Discussion started: 20 March 2025

595

Data availability: The datasets used and/or analyzed during the current study are available on reasonable request from the authors Caroline Leck (lina@misu.su.se), Jost Heintzenberg (jost@tropos.de), and Tuomas Naakka (tuomas.naakka@fmi.fi). The subset of observations from the 2018 expedition used in this study can be accessed through the Bolin Centre Database (https://doi.org/10.17043/ oden-ao-2018-aerosol-dmps-1, Karlsson and Zieger, 2020; https://doi.org/10.17043/oden-ao-2018-misu-weather-3.

Competing interests: The authors declare that they have no conflict of interest.

Disclaimer: Special issue statement: the statement on a corresponding special issue will be included by Copernicus, if applicable.

Author contribution: Caroline Leck – Conceptualization, Methodology, Validation, Formal analysis, Investigation, Resources, Writing - Original Draft, Writing - Review & Editing, Visualization, Project administration. **Jost Heintzenberg** – Methodology, Validation, Formal analysis, Data Curation, Writing - Original Draft, Writing - Review & Editing, Visualization. **Tiina Nygård** – Validation, Formal analysis, Data Curation, Writing – Parts of Original Draft Writing - Review & Editing, Visualization. **Tuomas Naakka** – Data Curation, Writing – Parts of Original Draft, Writing - Review & Editing.

Acknowledgments: We thank John Ogren for his generous assistance in acquiring the 2023 ice data following a significant alteration in the NSIDC file structure. We thank Pasi P. Aalto, Douglas Orsini, Paul Zieger, and Andreas Baccarini for their dedicated efforts in physical aerosol data collection and quality assurance. We acknowledge the Swedish Polar Research Secretariat (SPRS) for facilitating access to the Swedish icebreaker *Oden* and providing logistical support. Finally, we wish to convey our deep appreciation to the Captains of the *Oden* during the five research expeditions in 1991, 1996, 2001, 2008, and 2018: Anders Backman, Mats Johansson, Mattias Peterson—and their exemplary crew for their invaluable assistance.

Financial support: This work was supported by the International Meteorological Institute (IMI), the Swedish Research Council (VR), the Knut and Alice Wallenberg Foundation, and the Bolin Centre for Climate Research at Stockholm University.

Review statement: the review statement will be included by Copernicus.

https://doi.org/10.5194/egusphere-2025-695
Preprint. Discussion started: 20 March 2025

References

Alexander, L. V., Uotila, P., Nicholls, N., and Lynch, A.: A New Daily Pressure Dataset for Australia and Its Application to the Assessment of Changes in Synoptic Patterns during the Last Century, J. Clim., 23, 1111-1126, 10.1175/2009jcli2972.1, 2010.

Alvarez-Aviles, L., Simpson, W. R., Douglas, T. A., Sturm, M., Perovich, D., and Domine, F.: Frost flower chemical composition during growth and its implications for aerosol production and bromine activation, J. Geophys. Res., 113, https://doi.org/10.1029/2008JD010277, 2008.

Andrea, R., Christine, M., Michel, G., and Bernard, L.: Enrichment of nutrients, exopolymeric substances and microorganisms in newly formed sea ice on the Mackenzie shelf, Mar. Ecol. Prog. Ser., 342, 55-67, 2007.

Arrigo, K. R., Perovich, D. K., Pickart, R. S., Brown, Z. W., van Dijken, G. L., Lowry, K. E., Mills, M. M., Palmer, M. A., Balch, W. M., Bahr, F., Bates, N. R., Benitez-Nelson, C., Bowler, B., Brownlee, E., Ehn, J. K., Frey, K. E., Garley, R., Laney, S. R., Lubelczyk, L., Mathis, J., Matsuoka, A., Mitchell, B. G., Moore, G. W. K., Ortega-Retuerta, E., Pal, S., Polashenski, C. M., Reynolds, R. A., Schieber, B., Sosik, H. M., Stephens, M., and Swift, J. H.: Massive Phytoplankton Blooms Under Arctic Sea Ice, Science, 336, 1408-1408, doi:10.1126/science.1215065, 2012.

Aslam, S. N., Michel, C., Niemi, A., and Underwood, G. J. C.: Patterns and drivers of carbohydrate budgets in ice algal assemblages from first year Arctic sea ice, Limnol. Oceanogr., 61, 919-937, https://doi.org/10.1002/lno.10260, 2016.

Baccarini, A., Karlsson, L., Dommen, J., Duplessis, P., Vüllers, J., Brooks, I. M., Saiz-Lopez, A., Salter, M., Tjernström, M.,

Baltensperger, U., Zieger, P., and Schmale, J.: Frequent new particle formation over the high Arctic pack ice by enhanced iodine emissions, Nature Communications, 11, 4924, 10.1038/s41467-020-18551-0, 2020.

Bigg, E. K., and Leck, C.: Cloud-active particles over the central Arctic Ocean, J. Geophys. Res., 106, 32,155-132,166, 2001.

Bigg, E. K., and Leck, C.: The composition of fragments of bubbles bursting at the ocean surface, J. Geophys. Res., 113, D11209, doi:11210.11029/12007JD009078, 2008.

https://doi.org/10.5194/egusphere-2025-695
Preprint. Discussion started: 20 March 2025

Bowman, J. S., and Deming, J. W.: Elevated bacterial abundance and exopolymers in saline frost flowers and implications for atmospheric chemistry and microbial dispersal, Geophysical Research Letters, 37, https://doi.org/10.1029/2010GL043020, 2010.

Carmack, E., and Wassmann, P.: Food webs and physical–biological coupling on pan-Arctic shelves: Unifying concepts and comprehensive perspectives, Progress in Oceanography, 71, 446-477, https://doi.org/10.1016/j.pocean.2006.10.004, 2006.

Comiso, J.: Fundamental Characteristics of the Polar Oceans and Their Sea Ice Cover, in: Polar Oceans from Space, Springer New York, New York, NY, 19-71, 2010.

Covert, D. S., Wiedensohler, A., Aalto, P., Heintzenberg, J., McMurry, P. H., and Leck, C.: Aerosol number size distributions from 3 to 500 nm diameter in the arctic marine boundary layer during summer and autumn, Tellus, 48B, 197-212, 1996.

Deming, J. W., and Young, J. N.: The Role of Exopolysaccharides in Microbial Adaptation to Cold Habitats, in: Psychrophiles: From Biodiversity to Biotechnology, edited by: Margesin, R., Springer International Publishing, Cham, 259-284, 2017.

Ewert, M., and Deming, J. W.: Sea Ice Microorganisms: Environmental Constraints and Extracellular Responses, Biology, 2, 603-628, 2013.

Galley, R. J., Else, B. G. T., Geilfus, N. X., Hare, A. A., Isleifson, D., Barber, D. G., and Rysgaard, S.: Imaged brine inclusions in young sea ice—Shape, distribution and formation timing, Cold Reg. Sci. Technol., 111, 39-48, https://doi.org/10.1016/j.coldregions.2014.12.011, 2015.

Good, S.: Global Ocean OSTIA Sea Surface Temperature and Sea Ice Analysis, EU Copernicus Marine Service Information (CMEMS), Marine Data Store (MDS), 2022.

Heintzenberg, J., Leck, C., Birmili, W., Wehner, B., Tjernström, M., and Wiedensohler, A.: Aerosol number-size distributions during clear and fog periods in the summer high Arctic: 1991, 1996, and 2001, Tellus, 58B, 41-50, 2006.

Heintzenberg, J., and Leck, C.: The summer aerosol in the central Arctic 1991 - 2008: did it change or not?, Atmos. Chem. Phys., 12, 3969-3983, 2012.

Heintzenberg, J., Leck, C., and Tunved, P.: Potential source regions and processes of aerosol in the summer Arctic, Atmos. Chem. Phys., 15, 6487-6502, 10.5194/acp-15-6487-2015, 2015.

https://doi.org/10.5194/egusphere-2025-695
Preprint. Discussion started: 20 March 2025

685 Held, A., Brooks, I. M., Leck, C., and Tjernström, M.: On the potential contribution of open lead particle emissions to the central Arctic aerosol concentration, Atmos. Chem. Phys., 11, 3093-3105, 10.5194/acp-11-3093-2011, 2011.

Hersbach, H., Bell, B., Berrisford, P., Hirahara, S., Horányi, A., Muñoz-Sabater, J., Nicolas, J., Peubey, C., Radu, R., Schepers, D., Simmons, A., Soci, C., Abdalla, S., Abellan, X., Balsamo, G., Bechtold, P., Biavati, G., Bidlot, J., Bonavita, M., De Chiara,
690 G., Dahlgren, P., Dee, D., Diamantakis, M., Dragani, R., Flemming, J., Forbes, R., Fuentes, M., Geer, A., Haimberger, L., Healy, S., Hogan, R. J., Hólm, E., Janisková, M., Keeley, S., Laloyaux, P., Lopez, P., Lupu, C., Radnoti, G., de Rosnay, P., Rozum, I., Vamborg, F., Villaume, S., and Thépaut, J.-N.: The ERA5 global reanalysis, Q. J. Roy. Meteorol. Soc., 146, 1999-2049, https://doi.org/10.1002/qj.3803, 2020.

695 Hersbach, H., Bell, B., Berrisford, P., Biavati, G., Horányi, A., Muñoz Sabater, J., Nicolas, J., Peubey, C., Radu, R., Rozum, I., Schepers, D., Simmons, A., Soci, C., Dee, D., Thépaut, J-N.: ERA5 hourly data on single levels from 1940 to present, Copernicus Climate Change Service (C3S) Climate Data Store (CDS), 10.24381/cds.adbb2d47, 2023, (last accessed 2024-10-31).

700 Hewitson, B. C., and Crane, R. G.: Self-organizing maps: applications to synoptic climatology, Climate Research, 22, 13-26, 2002.

Hezel, P. J., Zhang, X., Bitz, C. M., Kelly, B. P., and Massonnet, F.: Projected decline in spring snow depth on Arctic sea ice caused by progressively later autumn open ocean freeze-up this century, Geophysical Research Letters, 39,
705 https://doi.org/10.1029/2012GL052794, 2012.

Kanamitsu, M.: Description of the NMC Global Data Assimilation and Forecast System, Wea. Forecasting, 4, 335-342, 10.1175/1520-0434(1989)004<0335:DOTNGD>2.0.CO;2, 1989.

710 Karl, M., Leck, C., Gross, A., and Pirjola, L.: A Study of New Particle Formation in the Marine Boundary Layer Over the Central Arctic Ocean using a Flexible Multicomponent Aerosol Dynamic Model, Tellus, 64B, doi:http://dx.doi.org/10.3402/tellusb.v3464i3400.17158, 2012.

Karl, M., Leck, C., Coz, E., and Heintzenberg, J.: Marine nanogels as a source of atmospheric nanoparticles in the high Arctic,
715 Geophysical Research Letters, 40, 3738–3743, DOI: 10.1002/grl.50661, 2013.

https://doi.org/10.5194/egusphere-2025-695
Preprint. Discussion started: 20 March 2025

Karlsson, L., and Zieger, P.: Aerosol particle number size distribution data collected during the Arctic Ocean 2018 expedition, Bolin Centre Database, https://doi.org/10.17043/odenao-12018-aerosol-dmps-17041, 2020.

Kohonen, T.: Self-Organizing Maps, Springer-Verlag, 501 pp., 2001.

Krembs, C., Eicken, H., Junge, K., and Deming, J. W.: High concentrations of exopolymeric substances in Arctic winter sea ice: implications for the polar ocean carbon cycle and cryoprotection of diatoms, Deep Sea Research Part I: Oceanographic Research Papers, 49, 2163-2181, https://doi.org/10.1016/S0967-0637(02)00122-X, 2002.

Lange, B. A., Michel, C., Beckers, J. F., Casey, J. A., Flores, H., Hatam, I., Meisterhans, G., Niemi, A., and Haas, C.: Comparing Springtime Ice-Algal Chlorophyll a and Physical Properties of Multi-Year and First-Year Sea Ice from the Lincoln Sea, PLoS One, 10, e0122418, 10.1371/journal.pone.0122418, 2015.

Lawler, M. J., Saltzman, E. S., Karlsson, L., Zieger, P., Salter, M., Baccarini, A., Schmale, J., and Leck, C.: New Insights Into the Composition and Origins of Ultrafine Aerosol in the Summertime High Arctic, Geophys. Res. Lett., 48, e2021GL094395, https://doi.org/10.1029/2021GL094395, 2021.

Leck, C., Bigg, E. K., Covert, D. S., Heintzenberg, J., Maenhaut, W., Nilsson, E. D., and Wiedensohler, A.: Overview of the atmospheric research program during the International Arctic Ocean Expedition of 1991 (IAOE-91) and its scientific results, Tellus, 48B, 136-155, 1996.

Leck, C., and Persson, C.: Seasonal and short-term variability in dimethyl sulfide, sulfur dioxide and biogenic sulfur and sea salt aerosol particles in the arctic marine boundary layer, during summer and autumn, Tellus, 48B, 272-299, 1996.

Leck, C., and Bigg, E. K.: Aerosol production over remote marine areas - A new route, Geophys. Res. Lett., 23, 3577-3581, 1999.

Leck, C., Nilsson, E. D., Bigg, E. K., and Bäcklin, L.: The atmospheric program on the Arctic Ocean Expedition 1996 (AOE-96): An overview of scientific goals, experimental approach, and instruments, J. Geophys. Res., 106, 32051-32067, 2001.

Leck, C., Norman, M., Bigg, E. K., and Hillamo, R.: Chemical composition and sources of the high Arctic aerosol relevant for cloud formation, J. Geophys. Res., 107, doi:10.1029/2001JD001463., 2002.

https://doi.org/10.5194/egusphere-2025-695
Preprint. Discussion started: 20 March 2025

Leck, C., and Bigg, E. K.: Biogenic particles in the surface microlayer and overlaying atmosphere in the central Arctic Ocean during summer, Tellus, 57B, 305–316, 2005.

Leck, C., and Bigg, E. K.: New particle formation of marine biological origin, Aerosol Sci. Technol., 44, 570-577, 2010.

Leck, C., Gao, Q., Mashayekhy Rad, F., and Nilsson, U.: Size-resolved atmospheric particulate polysaccharides in the high summer Arctic, Atmos. Chem. Phys., 13, 12573-12588, 10.5194/acp-13-12573-2013, 2013.

Leck, C., and Svensson, E.: Importance of aerosol composition and mixing state for cloud droplet activation over the Arctic pack ice in summer, Atmos. Chem. Phys., 15, 2545-2568, 10.5194/acp-15-2545-2015, 2015.

Leck, C., Matrai, P., Perttu, A.-M., and Gårdfeldt, K., 2019, , Tech. rep., Swedish. Polar Research Secretariat, ISBN 978-91-519-3671-0, 2019: Expedition report: SWEDARTIC Arctic Ocean 2018, Swedish. Polar Research Secretariat, Stockholm, ISBN 978-991-519-3671-3670, 2019.

Matrai, P. A., Tranvik, L., Leck, C., and Knulst, J. C.: Are high Arctic surface-microlayers a potential source of aerosol organic precursors?, Mar. Chem., 108, 109-122, 2008.

Mauritsen, T., Sedlar, J., Tjernström, M., Leck, C., Martin, M., Shupe, M., Sjogren, S., Sierau, B., Persson, P. O. G., Brooks, I. M., and Swietlicki, E.: An Arctic CCN-limited cloud-aerosol regime, Atmos. Chem. Phys., 11, 165-173, 10.5194/acp-11-165-2011, 2011.

Meier, W. N., Hovelsrud, G. K., van Oort, B. E. H., Key, J. R., Kovacs, K. M., Michel, C., Haas, C., Granskog, M. A., Gerland, S., Perovich, D. K., Makshtas, A., and Reist, J. D.: Arctic sea ice in transformation: A review of recent observed changes and impacts on biology and human activity, Rev. Geophys., 52, 185-217, https://doi.org/10.1002/2013RG000431, 2014.

Mortin, J., Svensson, G., Graversen, R. G., Kapsch, M.-L., Stroeve, J. C., and Boisvert, L. N.: Melt onset over Arctic sea ice controlled by atmospheric moisture transport, Geophysical Research Letters, 43, 6636-6642, 10.1002/2016GL069330, 2016.

Nilsson, E. D., and Barr, S.: Effcts of synoptic patterns on atmospheric chemistry and aerosols during the Arctic Ocean Expedition 1996, J. Geophys. Res., 106, 32,069-032,086, 2001.

Nilsson, E. D., Rannik, Ü., Swietlicki, E., Leck, C., Aalto, P. P., Zhou, J., and Norman, M.: Turbulent aerosol fluxes over the Arctic Ocean 2. Wind-driven sources from the sea, J. Geophys. Res., 106, 32,139-132,154, 2001.

https://doi.org/10.5194/egusphere-2025-695
Preprint. Discussion started: 20 March 2025

Nilsson, E. D., and Leck, C.: A pseudo-Lagrangian study of the sulfur budget in the remote Arctic marine boundary layer, Tellus B, 54, 213-230, 2002.

Nygård, T., Graversen, R. G., Uotila, P., Naakka, T., and Vihma, T.: Strong Dependence of Wintertime Arctic Moisture and Cloud Distributions on Atmospheric Large-Scale Circulation, J. Clim., 32, 8771-8790, https://doi.org/10.1175/JCLI-D-19-0242.1, 2019.

Nygård, T., Tjernström, M., and Naakka, T.: Winter thermodynamic vertical structure in the Arctic atmosphere linked to large-scale circulation, Weather Clim. Dynam., 2, 1263-1282, 10.5194/wcd-2-1263-2021, 2021.

Olli, K., Wassmann, P., Reigstad, M., Ratkova, T. N., Arashkevich, E., Pasternak, A., Matrai, P. A., Knulst, J., Tranvik, L., Klais, R., and Jacobsen, A.: The fate of production in the central Arctic Ocean – top–down regulation by zooplankton expatriates?, Progress in Oceanography, 72, 84-113, https://doi.org/10.1016/j.pocean.2006.08.002, 2007.

Orellana, M. V., Matrai, P. A., Leck, C., Rauschenberg, C. D., Lee, A. M., and Coz, E.: Marine microgels as a source of cloud condensation nuclei in the high Arctic, Proceedings of the National Academy of Sciences, 108, 13612–13617, 2011.

Orellana, M. V., Hansell, D. A., Matrai, P. A., and Leck, C.: Marine Polymer-Gels' Relevance in the Atmosphere as Aerosols and CCN, Gels, 7, 185, 2021.

Perovich, D. K., and Richter-Menge, J. A.: Surface characteristics of lead ice, Journal of Geophysical Research: Oceans, 99, 16341-16350, https://doi.org/10.1029/94JC01194, 1994.

Polyakov, I. V., Ingvaldsen, R. B., Pnyushkov, A. V., Bhatt, U. S., Francis, J. A., Janout, M., Kwok, R., and Skagseth, Ø.: Fluctuating Atlantic inflows modulate Arctic atlantification, Science, 381, 972-979, doi:10.1126/science.adh5158, 2023.

Rantanen, M., Karpechko, A. Y., Lipponen, A., Nordling, K., Hyvärinen, O., Ruosteenoja, K., Vihma, T., and Laaksonen, A.: The Arctic has warmed nearly four times faster than the globe since 1979, Communications Earth & Environment, 3, 168, 10.1038/s43247-022-00498-3, 2022.

Riedel, A., Michel, C., Gosselin, M., and LeBlanc, B.: Enrichment of nutrients, exopolymeric substances and microorganisms in newly formed sea ice on the Mackenzie shelf, Mar. Ecol. Prog. Ser., 342, 55-67, 2007.

https://doi.org/10.5194/egusphere-2025-695
Preprint. Discussion started: 20 March 2025

Rigor, I. G., Colony, R. L., and Martin, S.: Variations in Surface Air Temperature Observations in the Arctic, 1979–97, J. Clim., 13, 896-914, https://doi.org/10.1175/1520-0442(2000)013<0896:VISATO>2.0.CO;2, 2000.

Saiz-Lopez, A., Blaszczak-Boxe, C. S., and Carpenter, L. J.: A mechanism for biologically induced iodine emissions from sea ice, Atmos. Chem. Phys., 15, 9731-9746, 10.5194/acp-15-9731-2015, 2015.

Salter, M. E., Hamacher-Barth, E., Leck, C., Werner, J., Johnson, C. M., Riipinen, I., Nilsson, E. D., and Zieger, P.: Calcium enrichment in sea spray aerosol particles, Geophys. Res. Lett., 43, 8277-8285, https://doi.org/10.1002/2016GL070275, 2016.

Stein, A. F., Draxler, R. R., Rolph, G. D., Stunder, B. J. B., Cohen, M. D., and Ngan, F.: NOAA's HYSPLIT Atmospheric Transport and Dispersion Modeling System, Bull. Amer. Meteor. Soc., 96, 2059-2077, 10.1175/BAMS-D-14-00110.1, 2015.

Thomas, D. N., S. Papadimitriou, and C. Michel.: Biogeochemistry of sea ice, in, edited by: Thomas, D. N., and Dieckmann, G. S., Wiley-Blackwell, 425–468., 2010.

Thomas, M. A., Devasthale, A., and Nygård, T.: Influence of springtime atmospheric circulation types on the distribution of air pollutants in the Arctic, Atmos. Chem. Phys., 21, 16593-16608, 10.5194/acp-21-16593-2021, 2021.

Thomdike, A. S., and Cheung, J. Y.: A IDJEX measurements of sea ice motion 11 April 1975 to 14 May 1976, AIDJEX Bull., 35, 1-149, 1977.

Timmermans, M.-L., and Marshall, J.: Understanding Arctic Ocean Circulation: A Review of Ocean Dynamics in a Changing Climate, Journal of Geophysical Research: Oceans, 125, e2018JC014378, https://doi.org/10.1029/2018JC014378, 2020.

Titchner, H. A., and Rayner, N. A.: The Met Office Hadley Centre sea ice and sea surface temperature data set, version 2: 1. Sea ice concentrations, J. Geophys. Res., 119, 2864-2889, https://doi.org/10.1002/2013JD020316, 2014.

Tjernström, M., Leck, C., Persson, P. O. G., Jensen, M. L., Oncley, S. P., and Targino, A.: Experimental Equipment: A Supplement to "The Summertime Arctic Atmosphere: Meteorological Measurements during the Arctic Ocean Experiment 2001", Bull. Amer. Meteor. Soc., 85, 1322-1326, 2004.

Tjernström, M., Birch, C., Brooks, I., Leck, C., Mauritsen, T., Paatero, J., Persson, O., Sedlar, J., Shupe, M., Szczodrak, M., and Wheeler, C.: Central Arctic atmospheric conditions during the Arctic Summer Cloud Ocean Study (ASCOS) field phase: Contrasting to previous expeditions, Atmos. Chem. Phys., 12, 6863–6889, 2012.

https://doi.org/10.5194/egusphere-2025-695
Preprint. Discussion started: 20 March 2025

Tjernström, M., Leck, C., Birch, C. E., Bottenheim, J. W., Brooks, B. J., Brooks, I. M., Bäcklin, L., Chang, R. Y.-W., Granath, E., Graus, M., Hansel, A., Heintzenberg, J., Held, A., Hind, A., Rosa, S. d. l., Johnston, P., Knulst, J., Westberg, M., Leeuw, G. d., Liberto, L. D., Martin, M., Matrai, P. A., Mauritsen, T., Müller, M., Norris, S. J., Orellana, M. V., Orsini, D. A., Paatero, J., Persson, P. O. G., Gao, Q., Rauschenberg, C., Ristovski, Z., Sedlar, J., Shupe, M. D., Sierau, B., Anders, Sirevaag, Sjogren, S., Stetzer, O., Swietlicki, E., Szczodrak, M., Vaattovaara, P., Wahlberg, N., and Wheeler, C. R.: The Arctic Summer Cloud-Ocean Study (ASCOS): Overview and experimental design, Atmos. Chem. Phys., 14, 2823-2869, 2014.

Vancoppenolle, M., Meiners, K. M., Michel, C., Bopp, L., Brabant, F., Carnat, G., Delille, B., Lannuzel, D., Madec, G., Moreau, S., Tison, J.-L., and van der Merwe, P.: Role of sea ice in global biogeochemical cycles: emerging views and challenges, Quat. Sci. Rev., 79, 207-230, https://doi.org/10.1016/j.quascirev.2013.04.011, 2013.

Wassmann, P., and Reigstad, M.: Future Arctic Ocean Seasonal Ice Zones and Implications for Pelagic-Benthic Coupling, Oceanography, 24, 220-231, 2011.

Whitby, E., and McMurry, P. H.: Modal aerosol dynamics modeling, Aerosol Sci. Technol., 27, 673-688, 1997.